

Revisiting energy-efficient hybrid and digital beamforming architectures above 100 GHz

Yiğit Ertuğrul

ESAT KU Leuven, Kasteelpark Arenberg
imec, Kapeldreef 75
3001 Leuven - Belgium
Yigit.Ertugrul@imec.be

Claude Desset

imec, Kapeldreef 75
3001 Leuven - Belgium
desset@imec.be

Sofie Pollin

ESAT KU Leuven, Kasteelpark Arenberg
imec, Kapeldreef 75
3001 Leuven - Belgium
sofie.pollin@kuleuven.be

Abstract—Millimeter-wave spectrum (30 to 300 GHz) is explored in order to provide higher throughput by exploiting the large bandwidth available. At those frequencies, multiple antenna systems are essential to combat severe path loss. Fully digital (FD) architectures, where each antenna connects to its own baseband chain, are considered the most energy-efficient at low frequencies while enabling multi-user multiplexing. However, unlike lower frequencies, channel propagation above 100 GHz is heavily line-of-sight dominated and the operating bandwidth is much larger which poses different constraints on signaling schemes and hardware components. The optimal beamforming architecture configuration is still an open problem above 100 GHz. To address this problem, we compare energy-efficient beamforming architectures for the D-band (110-170 GHz). We estimate the energy efficiency of future systems by following the technology trends in circuit implementation. We show that hybrid fully connected architecture is the most energy-efficient for the 7nm technology node and size-constrained antenna arrays. Hybrid partially connected architecture is the most energy-efficient for unconstrained antenna arrays. We show that FD architecture becomes energy-efficient for technology nodes better than 2nm.

Index Terms—energy efficiency, beamforming, sub-THz

I. INTRODUCTION

Millimeter-wave (mm-wave) (30 to 300 GHz) spectrum has been explored to address the ever-increasing throughput requirement [1], [2]. At those frequencies, multiple-antenna technologies are the key enablers to combat severe path loss. The throughput demand can be addressed by designing systems with higher bandwidth. Therefore, industry and academia focused on D-band (110-170 GHz) where more than 10 GHz of contiguous bandwidth is available. Compared to lower frequencies, D-band restricts the channel propagation to single-stream per user for reliable communication [3], [4]. On the other hand, the power budget of the communication systems grows for future systems due to the increasing transmit power and the increasing baseband processing. Therefore, there is a transceiver architecture design challenge for future communication systems for improving the throughput with manageable power consumption.

Unlike fully digital (FD) architecture where each antenna has a dedicated digital chain, hybrid architectures are proposed to reduce the baseband processing complexity by connecting multiple antennas to a single digital chain. Hybrid and FD

architectures are compared in the literature from hardware complexity, algorithm complexity, energy efficiency, and spectral efficiency perspective. However, the operating frequency, channel characteristics, and hardware models alter the favorable architecture type depending on the constraints.

The sum-rate difference between hybrid fully connected (HFC) and hybrid partially connected (HPC) architectures is $K \log_2(K)$ for high signal-to-noise ratios where K is the number of users in [5]. The analysis draws theoretical conclusions neglecting hardware constraints. Based on a channel model dedicated to the lower part of the mm-wave spectrum, the double-phase shifter architecture is more spectrally efficient than HFC and HPC architectures in [6], but the study neglects the power analysis of hybrid architectures. A hybrid beamforming methodology is developed to maximize the energy efficiency and spectral efficiency in [7] where FD architecture is the most energy-efficient for an increasing number of users. Although HPC has simpler hardware, it cannot be more energy-efficient than FD due to lower spectral efficiency. The conclusions of this study are based on a simple hardware model and frequency agnostic channel model. Millimeter-wave beamforming architectures have been compared in [8] considering realistic use cases and hardware models. The analysis has been extended to practical system realization. The authors identified the FD architecture as the most power-efficient considering the urban microcell network use case. However, this study considers the lower part of the mm-wave spectrum where the results highly depend on the operating bandwidth, mm-wave channel, and power models. The conclusions are subject to change towards frequencies above 100 GHz. In [9], the authors studied the cost of splitter and insertion losses in hybrid architectures where the FD architecture can become favorable with reduced converter resolution. However, the conclusions are limited to dedicated hardware models and small operating bandwidth at 28 GHz. Considering the initial beam acquisition performance, HPC architecture outperforms HFC architecture in terms of hardware complexity and power efficiency in [10]. The statistics of the channel model are tailored to 40 GHz which differs significantly for a system operating above 100 GHz.

Moving to higher frequencies, at 60 GHz, HPC is the most energy-efficient architecture when there are a few users

(less interference suppression needed) [11]. On the other hand, FD architecture is favorable when the number of users increases. In [12], the authors set the analysis framework for future 6G systems with up-to-date hardware models. The authors studied link budget requirements for future cellular networks. However, the final analysis is limited to HPC, neglecting the HFC architecture. The authors in [13] identified the HPC as the most energy-efficient architecture considering sub-THz analog models. However, the evaluation has been done considering an oversimplified baseband power model. The power consumption of an FD receiver at 140 GHz is analyzed and the RF power consumption is optimized to consume less than 2W [14]. While optimizing relevant RF components and digital processing, this study neglects the contribution of baseband power consumption. Considering the THz spectrum (0.1-1 THz), the authors have identified channel sparsity and low spatial degrees of freedom (SDoF) as one of the challenges from the THz channel perspective and propose to use widely-spaced arrays to overcome the low (SDoF) problem [15]. They conclude that the power consumption of the HFC architecture is unacceptably high due to the excessive use of phase shifters. All the works mentioned above are either targeting lower frequencies having different power models and channel characteristics or provide an incomplete energy efficiency analysis of beamforming architectures for sub-THz frequencies.

On top of the existing studies in the literature, we revisit the beamforming architecture comparison in the context of the D-band propagation conditions and power modeling. Our contributions are listed below,

- This paper is the first to compare the FD and hybrid beamforming architecture tradeoffs in terms of energy efficiency with D-band channel models and models of the hardware power consumption.
- We use technology scaling to predict energy-efficient architectures for future systems.
- This paper shows that the HFC is the most energy-efficient architecture up to 150 transmit antennas.
- We show that FD architecture becomes energy-efficient for technology nodes better than 2nm with 6 GHz bandwidth.
- This paper shows that HPC is the most energy-efficient architecture for extremely large antenna arrays.

The rest of the paper is organized as follows. In Section II, we explain the system model along with the link budget and power model. The energy efficiency of hybrid and FD architectures are analyzed in Section III, where we discuss a multi-user use case targeting high data rates. We finalize the analysis in Section IV.

II. SYSTEM MODEL

We model a base station (BS) with N_{BS} antennas serving K users having N_{UE} antennas each. We restrict ourselves to single data stream per user due to channel properties above 100 GHz frequencies. Let s_k denote the data symbol transmitted to

user k and $\mathbf{s} = [s_1, s_2, \dots, s_K]$ denote the combined data symbols. We assume data symbols are normalized by the number of users and symbols between different users are uncorrelated i.e., $\mathbb{E}[\mathbf{s}^H \mathbf{s}] = \frac{1}{K}$. Prior to transmission data symbols are precoded by the precoding matrix $\mathbf{F} = [\mathbf{f}_1, \mathbf{f}_2, \dots, \mathbf{f}_K] \in \mathbb{C}^{N_{BS} \times K}$. We limit the transmission power by $|\mathbf{F}|^2 \leq K$. The transmitted signal from antennas is $\mathbf{x} = \mathbf{F}\mathbf{s}$. Let $\mathbf{H}_k \in \mathbb{C}^{N_{UE} \times N_{BS}}$ denote the channel between the BS and user k . We use the geometric sub-THz channel model [3],

$$\mathbf{H}_k = \sqrt{\frac{N_{BS}N_{UE}}{L}} \sum_{l=1}^L a_l \mathbf{a}_R(\theta_l^R, \phi_l^R) \mathbf{a}_T^H(\theta_l^T, \phi_l^T) \quad (1)$$

where L is the number of propagation paths, a_l is the complex path gain, θ_l^R and ϕ_l^R are the angle of arrival (AOA) for path l in azimuth and elevation, respectively. θ_l^T and ϕ_l^T are the angle of departure (AOD) for path l in azimuth and elevation, respectively. We consider uniform planar arrays (UPA) at the BS and user terminals with $\lambda/2$ spacing between different elements. We refer readers to [3] for the detailed description of a_l , $\mathbf{a}_R(\theta_l^R, \phi_l^R)$, and $\mathbf{a}_T(\theta_l^T, \phi_l^T)$.

The received signal at user antennas can be written as $\mathbf{r}_k = \mathbf{H}_k \mathbf{x} + \mathbf{n}$ where $\mathbf{n} \sim \mathcal{CN}(0, \sigma^2 \mathbf{I}_{N_{UE}}) \in \mathbb{C}^{N_{UE} \times 1}$ is the additive noise. We can express the received signal as desired signal, interference signal and noise,

$$\mathbf{r}_k = \mathbf{H}_k \mathbf{f}_k s_k + \sum_{n=1|n \neq k}^K \mathbf{H}_k \mathbf{f}_n s_n + \mathbf{n} \quad (2)$$

User k further processes the received signal by combining with its own combining vector $\mathbf{w}_k \in \mathbb{C}^{N_{UE} \times 1}$,

$$y_k = \mathbf{w}_k^H \mathbf{r}_k = \mathbf{w}_k^H \mathbf{H}_k \mathbf{f}_k s_k + \mathbf{w}_k^H \sum_{n=1|n \neq k}^K \mathbf{H}_k \mathbf{f}_n s_n + \mathbf{w}_k^H \mathbf{n}, \quad (3)$$

where $\mathbf{w}_k^H \mathbf{w}_k = 1$. The spectral efficiency of user k is calculated by

$$R_k = \log_2 \left(1 + \frac{\gamma_k |\mathbf{w}_k^H \mathbf{H}_k \mathbf{f}_k|^2}{\gamma_k \sum_{i=1|i \neq k}^K |\mathbf{w}_k^H \mathbf{H}_k \mathbf{f}_i|^2 + 1} \right), \quad (4)$$

where $\gamma_k = \frac{N_{BS} P_{PA}^{(out)}}{K \sigma^2}$ is the signal-to-noise ratio and $P_{PA}^{(out)}$ is the output power of a single power amplifier.

A. Link budget

Equivalent isotropically radiated power (EIRP) of stream k towards (θ, ϕ) direction can be calculated as [16]

$$\text{EIRP}(\theta, \phi)_k = \frac{N_{BS}}{K} P_{PA}^{(out)} |\mathbf{a}_T^H(\theta, \phi) \mathbf{f}_k|^2. \quad (5)$$

The total EIRP in (θ, ϕ) direction can be calculated as $\sum_{k=1}^K \text{EIRP}(\theta, \phi)_k$. The average received desirable signal power of user k after combining can be written by

$$P_k = \frac{N_{BS}}{K} P_{PA}^{(out)} \mathbb{E} [|\mathbf{w}_k^H \mathbf{H}_k \mathbf{f}_k|^2], \quad (6)$$

where $\mathbb{E}[\cdot]$ is the expected value. The interference signal power of user k

$$I_k = \frac{N_{BS}}{K} P_{PA}^{(out)} \sum_{n=1|n \neq k}^K \mathbb{E} \left[|\mathbf{w}_k^H \mathbf{H}_k \mathbf{f}_n|^2 \right] \quad (7)$$

Noise power is related to the operating bandwidth as $P_N = KTB + F_{LNA}$ where KTB is the thermal noise power and F_{LNA} is the noise figure of the low-noise amplifier at the user terminal. Signal to interference noise ratio (SINR) for user k is calculated by $\beta_k = \frac{P_k}{I_k + P_N}$. We approximate the achieved downlink throughput for user k as

$$T_k = \frac{2}{3} B \log_2(1 + \beta_k), \quad (8)$$

where we inspire from the channel capacity formula and scale it to approximate the implementation losses.

B. Hybrid architectures

The precoding matrix for hybrid architectures can be characterized more by factorizing the precoding matrix into RF and baseband parts i.e., $\mathbf{F} = \mathbf{F}_{RF} \mathbf{F}_{BB}$ where $\mathbf{F}_{RF} = [\mathbf{f}_{RF,1} \ \mathbf{f}_{RF,2} \ \dots \ \mathbf{f}_{RF,K}] \in \mathbb{C}^{N_{BS} \times K}$ and $\mathbf{F}_{BB} \in \mathbb{C}^{K \times K}$. In this study, we consider baseband precoders of size $K \times K$ where the number of RF chains is limited by the number of users for hybrid architectures. Please note that each element of the RF precoding matrix is either phase shift or zero depending on the hybrid architecture type. HFC architecture can be realized by having non-zero elements in \mathbf{F}_{RF} i.e., $f_{ik} = \frac{e^{j\theta_{ik}}}{\sqrt{N_{BS}}}$, $f_{ik} \neq 0$ where all RF chains are connected to all antennas. HPC architecture can be realized by having a block diagonal \mathbf{F}_{RF} where each RF chain is connected to different $M_{BS} = \frac{N_{BS}}{K}$ antennas, i.e., $f_{ik} = \frac{e^{j\theta_{ik}}}{\sqrt{M_{BS}}}$. The same architectures can be used at the user terminal having $\mathbf{w}_k = \mathbf{w}_{RF,k} w_{BB,k}$, where $w_{BB,k}$ is a scalar. We follow a two-step approach in the hybrid precoder design [17] i.e., in the first step we design the RF precoder \mathbf{F}_{RF} and RF combiner $\mathbf{w}_{RF,k}$ for each user and in the second step we design the baseband precoder \mathbf{F}_{BB} . The RF precoder and combiner are designed as the following

$$\left\{ \mathbf{f}_{RF,k}^*, \mathbf{w}_{RF,k}^* \right\} = \arg \max |\mathbf{w}_{RF,k}^H \mathbf{H}_k \mathbf{f}_{RF,k}|^2, \quad (9)$$

where $\mathbf{w}_{RF,k} \in \mathcal{W}$ and $\mathbf{f}_{RF,k} \in \mathcal{F}$. Here \mathcal{W} and \mathcal{F} correspond to RF combining and precoding codebooks, respectively. In this work, we consider infinitely large codebooks. In the second step, we work on the equivalent channel that is seen by the digital baseband i.e., $\bar{\mathbf{H}}_k = \mathbf{w}_{RF,k}^H \mathbf{H}_k \mathbf{f}_{RF,k}$, to design the baseband precoder \mathbf{F}_{BB} . We construct the aggregate equivalent matrix by $\bar{\mathbf{H}} = [\bar{\mathbf{H}}_1^T \ \bar{\mathbf{H}}_2^T \ \dots \ \bar{\mathbf{H}}_K^T]^T$. The baseband precoder is calculated by

$$\mathbf{F}_{BB} = \bar{\mathbf{H}}^H (\bar{\mathbf{H}} \bar{\mathbf{H}}^H)^{-1}. \quad (10)$$

As a special case, we are interested in the spectral efficiency of the analog fully connected (AFC) and analog partially connected (APC) architectures having $\mathbf{F}_{BB} = \mathbf{I}_K$ to identify the effect of interference cancellation in hybrid architectures.

C. Power model

The power consumption of fully digital and hybrid architectures are listed in Table I. The transmit power consumption is analyzed as analog and digital circuits. The analog

TABLE I
TRANSMIT POWER CONSUMPTION OF DIFFERENT ARCHITECTURES

Architecture	P_{TX}
FD	$N_{BS} \left(P_{PA,DC}^{(out)} + P_{DAC} + P_{mix} + P_{LO,d} \right) + P_{LO} + P_{BB,dig}$
HFC	$N_{BS} \left(P_{PA,DC}^{(out)} + K P_{PS} + P_{mix} + P_{LO,d} \right) + K \left(P_{DAC} + P_{amp} \right) + P_{BB,hyb} + P_{LO}$
HPC	$N_{BS} \left(P_{PA,DC}^{(out)} + P_{PS} + P_{mix} + P_{LO,d} \right) + K \left(P_{DAC} + P_{amp} \right) + P_{BB,hyb} + P_{LO}$

section contains PA $P_{PA,DC}^{(out)} = P_{PA}^{(out)}/\eta$, mixer P_{mix} , local oscillator (LO) P_{LO} with its distribution $P_{LO,d}$, phase shifter P_{PS} , and digital-to-analog converter (DAC) P_{DAC} components. The digital section contains channel encoding, constellation mapping, IFFT, MIMO precoding, and upsampling & filtering operations. We use the reference values from [18] for the power consumption of individual analog components and digital blocks.

FD architecture does not have analog phase shifters since the phase of the signal is shifted digitally for each antenna output. However, digitally phase shifting the signal at each antenna increases the baseband power consumption significantly. Hybrid architectures utilize analog splitters to distribute the baseband signal to multiple antennas. The splitters degrade the signal power depending on the splitting ratio and the additional signal power is lost due to non-ideal hardware. The signal losses must be compensated by utilizing line amplifiers when needed to maintain the same signal level prior to splitting. We determine the required amplification following a similar approach to [8] and [13]. We compute the required amplification P_L as the following

$$P_L = \begin{cases} 10 \log_{10} N_{BS} + IL_s \log_2 N_{BS}, & HFC \\ 10 \log_{10} M_{BS} + IL_s \log_2 M_{BS}, & HPC \end{cases} \quad (11)$$

where IL_s is the insertion loss of the splitter. We assume that a signal is split into two having $\log_2 N_{BS}$ and $\log_2 M_{BS}$ stages for HFC and HPC, respectively. The DC power consumed by the line amplifiers is denoted by P_{amp} which corresponds to the power required to compensate P_L per baseband signal.

The baseband power consumption of the FD architecture P_{BB} scales with the number of antennas N_{BS} while the baseband power consumption of the hybrid architectures P_{BB} scale with the number of users K . Baseband power consumption P_{BB} is computed by counting the giga operations per second (GOPS) for each baseband function. We translate GOPS to Watts considering the implementation technology. We scale the baseband power consumption for future generations following the trends in CMOS technology [19]. We consider two production years 2022 and 2028 corresponding to 7nm and

2nm technology nodes, respectively to highlight the impact of circuit technology on energy efficiency.

III. ENERGY EFFICIENCY AND THROUGHPUT ANALYSIS

Energy efficiency at the transmit phase can be calculated as

$$E = \frac{P_{TX}}{\sum_{k=1}^K T_k}. \quad (12)$$

We decide on the most energy-efficient beamforming architecture by averaging the energy efficiency over many channel realizations. We focus on the urban microcell network use case where beamforming and corresponding architectures are essential since we are serving multiple users each demanding a high data rate. Table II summarizes the use case parameters where the maximum communication distance is limited by 70 meters and the propagation is mostly line of sight.

TABLE II
URBAN MICROCELL NETWORK USE CASE PARAMETERS

Parameter	Value
Frequency [GHz]	140
Bandwidth B [GHz]	6, 12
Number of users K	8
Maximum distance [m]	70
BS height [m]	10 [20]
Maximum EIRP [dBm]	70 [20]
Number of user antennas N_{UE}	16
$P_{PA}^{(out)}$ [dBm]	14
LNA noise figure F_{LNA} [dB]	5
Minimum average throughput per user [Gbps]	20

We target improving the data rate 10 times over 5G (20 Gbps per user) while serving 8 users ($K = 8$) simultaneously. The maximum EIRP is limited by 70 dBm at a given direction by the regulations of ITU [20]. We set the sub-THz channel model parameters such as L and a_l according to measurements based on [3]. Figure 1 illustrates the average throughput for FD, HFC, and HPC architectures on the left and the average spectral efficiency per user for FD, HFC, HPC, AFC, and APC architectures versus the number of BS antennas on the right. Due to channel sparsity, the FD and HFC architectures support the same throughput. This is in line with the results in [15], [17]. HPC architecture requires approximately 2.5 times more antennas to support the same throughput as HFC due to reduced EIRP. At 6 GHz operating bandwidth, FD and HFC architectures require at least 150 transmit antennas while HPC requires at least 350 antennas in order to satisfy the 20 Gbps average throughput per user. Doubling the operating bandwidth to 12 GHz reduces the minimum number of transmit antennas to 100 for FD and HFC architectures and 256 for HPC architecture. We investigate the spectral efficiency difference between HFC and HPC architectures compared to their analog-only counterparts and we conclude that the baseband interference cancellation significantly improves the spectral efficiency.

Average energy efficiency versus the number of transmit antennas for FD, HFC, and HPC architectures are illustrated

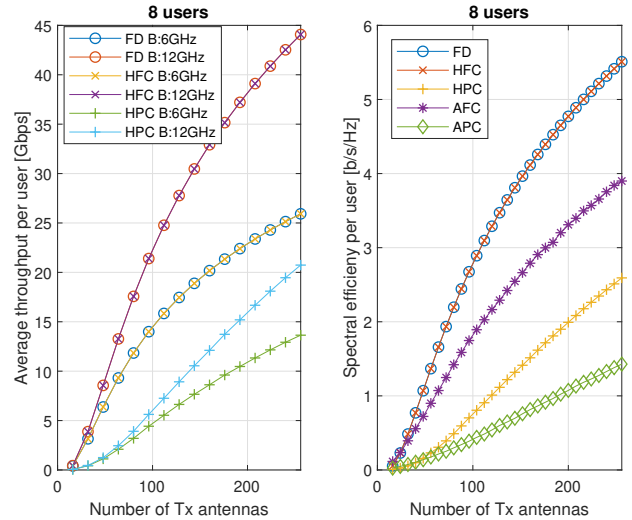


Fig. 1. Average throughput and spectral efficiency per user versus the number of transmit antennas. Average throughput per user comparison of FD, HFC, and HPC architectures for 6 and 12 GHz bandwidth on the left. Spectral efficiency per user comparison of FD, HFC, HPC, AFC, and APC architectures on the right.

in Fig. 2 where the number of users K equals 8 and operating bandwidth B equals 6 GHz for production years 2022 (7nm) and 2028 (2nm). For the 7nm technology node, HFC

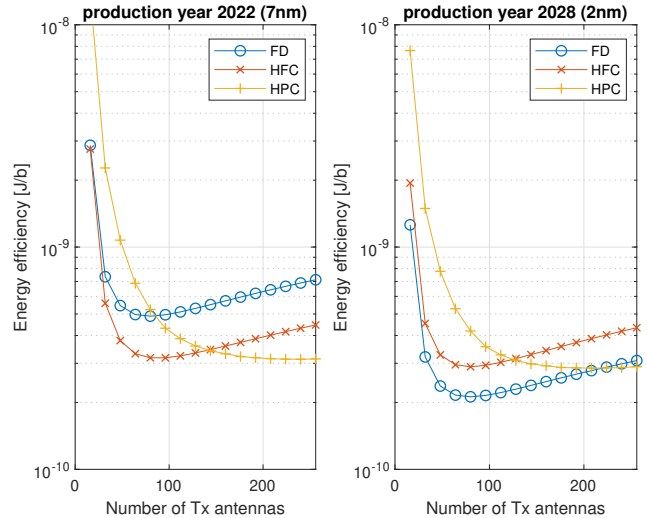


Fig. 2. Average energy efficiency versus the number of transmit antennas for 8 users, 6 GHz bandwidth, and the production years 2022 (7nm) and 2028 (2nm).

outperforms the FD architecture in all cases since it supports the same throughput with reduced power consumption. Furthermore, HFC is more energy-efficient than the HPC with up to 150 transmit antennas. HPC becomes the most energy-efficient architecture when the number of transmit antennas is greater than 150 due to high splitter losses in HFC. Improving the technology node to 2nm, FD outperforms the HFC and

HPC architectures for the values of N_{BS} less than 200 due to reduced baseband power consumption. We observe that FD architecture benefits from technology scaling more since P_{TX} is dominated by digital components. Average energy efficiency versus the number of transmit antennas for FD, HFC, and HPC architectures are illustrated in Fig. 3 where the number of users K equals 8 and operating bandwidth B equals 12 GHz for production years 2022 (7nm) and 2028 (2nm). Please note

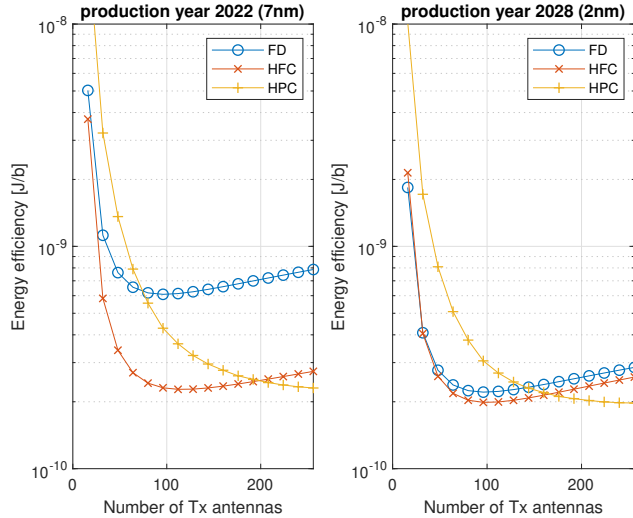


Fig. 3. Average energy efficiency versus the number of transmit antennas for 8 users, 12 GHz bandwidth, and the production years 2022 and 2028.

that FD cannot outperform the HFC architecture even for the technology node 2nm due to huge baseband complexity. HPC becomes more energy-efficient when N_{BS} is greater than 200 and 180 for the technology nodes 7nm and 2nm, respectively. HPC architecture becomes the most energy-efficient compared to FD and HFC architectures when there is no limit on the antenna array size due to a good enough spectral efficiency with many antennas while saving on power compared to other architectures. In order to satisfy the throughput requirement with a reasonable number of transmit antennas, we conclude that HFC architecture is the most energy-efficient architecture for the urban microcell network use case.

IV. CONCLUSION

We compared the energy efficiency of digital and hybrid beamforming architectures for frequencies above 100 GHz considering the D-band channel models and models of the hardware power consumption. We identified that the most energy-efficient architecture changes with respect to bandwidth, technology, and antenna array size constraints. HFC architecture is the most energy-efficient architecture considering the 7nm technology node and size-constrained antenna arrays, while HPC architecture becomes more energy-efficient for large antenna arrays. FD architecture becomes the most energy-efficient for the 2nm technology node and 6 GHz bandwidth with size-constrained antenna arrays.

REFERENCES

- [1] ETSI, "TS 138.211 Physical channels and modulation," *3rd Generation Partnership Project; Technical Specification Group Radio Access Network*.
- [2] IEEE, "IEEE Standard for Information technology–Telecommunications and information exchange between systems–Local and metropolitan area networks–Specific requirements–Part 11: Wireless LAN Medium Access Control (MAC) and Physical Layer (PHY) Specifications Amendment 3: Enhancements for Very High Throughput in the 60 GHz Band," *IEEE Std 802.11ad-2012 (Amendment to IEEE Std 802.11-2012, as amended by IEEE Std 802.11ae-2012 and IEEE Std 802.11aa-2012)*, pp. 1–628, 2012.
- [3] S. Ju and T. S. Rappaport, "Sub-Terahertz Spatial Statistical MIMO Channel Model for Urban Microcells at 142 GHz," in *2021 IEEE Global Communications Conference (GLOBECOM)*, 2021, pp. 1–6.
- [4] S. Ju, Y. Xing, O. Kanhere, and T. S. Rappaport, "Millimeter Wave and Sub-Terahertz Spatial Statistical Channel Model for an Indoor Office Building," *IEEE Journal on Selected Areas in Communications*, vol. 39, no. 6, pp. 1561–1575, 2021.
- [5] S. Wan, H. Zhu, K. Kang, and H. Qian, "On the Performance of Fully-Connected and Sub-Connected Hybrid Beamforming System," *IEEE Transactions on Vehicular Technology*, vol. 70, no. 10, pp. 11078–11082, 2021.
- [6] J. Zhang, X. Yu, and K. B. Letaief, "Hybrid Beamforming for 5G and Beyond Millimeter-Wave Systems: A Holistic View," *IEEE Open Journal of the Communications Society*, vol. 1, pp. 77–91, 2020.
- [7] K. Ardah, G. Fodor, Y. C. B. Silva, W. C. Freitas, and A. L. F. de Almeida, "Hybrid Analog-Digital Beamforming Design for SE and EE Maximization in Massive MIMO Networks," *IEEE Transactions on Vehicular Technology*, vol. 69, no. 1, pp. 377–389, 2020.
- [8] H. Yan, S. Ramesh, T. Gallagher, C. Ling, and D. Cabric, "Performance, Power, and Area Design Trade-Offs in Millimeter-Wave Transmitter Beamforming Architectures," *IEEE Circuits and Systems Magazine*, vol. 19, no. 2, pp. 33–58, 2019.
- [9] S. Dutta, C. N. Barati, D. Ramirez, A. Dhananjay, J. F. Buckwalter, and S. Rangan, "A Case for Digital Beamforming at mmWave," *IEEE Transactions on Wireless Communications*, vol. 19, no. 2, pp. 756–770, 2020.
- [10] X. Song, T. Kühne, and G. Caire, "Fully-/Partially-Connected Hybrid Beamforming Architectures for mmWave MU-MIMO," *IEEE Transactions on Wireless Communications*, vol. 19, no. 3, pp. 1754–1769, 2020.
- [11] S. Blandino, C. Desset, A. Bourdoux, and S. Pollin, "Energy Efficiency of Multiple-Input, Multiple-Output Architectures: Future 60-GHz Applications," *IEEE Vehicular Technology Magazine*, vol. 15, no. 2, pp. 65–71, 2020.
- [12] H. Halbauer and T. Wild, "Towards Power Efficient 6G Sub-THz Transmission," in *2021 Joint European Conference on Networks and Communications 6G Summit (EuCNC/6G Summit)*, 2021, pp. 25–30.
- [13] C. Lin and G. Y. Li, "Energy-Efficient Design of Indoor mmWave and Sub-THz Systems With Antenna Arrays," *IEEE Transactions on Wireless Communications*, vol. 15, no. 7, pp. 4660–4672, 2016.
- [14] P. Skrimponis, N. Hosseinzadeh, A. Khalili, E. Erkip, M. J. W. Rodwell, J. F. Buckwalter, and S. Rangan, "Towards Energy Efficient Mobile Wireless Receivers Above 100 GHz," *IEEE Access*, vol. 9, pp. 20704–20716, 2021.
- [15] C. Han, L. Yan, and J. Yuan, "Hybrid Beamforming for Terahertz Wireless Communications: Challenges, Architectures, and Open Problems," *IEEE Wireless Communications*, vol. 28, no. 4, pp. 198–204, 2021.
- [16] S. Dierks, "Multiple Antenna Precoding: Indoor Communications and EIRP," 2018.
- [17] A. Alkhateeb, G. Leus, and R. W. Heath, "Limited Feedback Hybrid Precoding for Multi-User Millimeter Wave Systems," *IEEE Transactions on Wireless Communications*, vol. 14, no. 11, pp. 6481–6494, 2015.
- [18] C. Desset, P. Wambacq, Y. Zhang, M. Ingels, and A. Bourdoux, "A flexible power model for mm-wave and THz high-throughput communication systems," in *2020 IEEE 31st Annual International Symposium on Personal, Indoor and Mobile Radio Communications*, 2020, pp. 1–6.
- [19] M. T. Bohr and I. A. Young, "CMOS Scaling Trends and Beyond," *IEEE Micro*, vol. 37, no. 6, pp. 20–29, 2017.
- [20] ITU, "Guidelines for evaluation of radio interface technologies for IMT-2020," ITU, Tech. Rep., 2017.